

Photonic crystal circuits: A theory for two- and three-dimensional networks

Arthur R. McGurn*

Department of Physics, Western Michigan University, Kalamazoo, Michigan 49008

(Received 13 July 1999; revised manuscript received 5 November 1999)

A discussion is given of waveguides in photonic crystals and branching network geometries of waveguides formed by joining several waveguide channels into conducting circuits for the transmission of light in photonic crystals. We shall refer to these structures in general as photonic crystal circuits. These conducting networks, which transport light, are an optical analogy to electrical circuits, which transport electrons through electrical networks. Photonic crystal circuits, however, unlike most electrical circuits, exhibit a variety of interference effects in their transport properties. The interference effects are related to the nondiffusive nature of the optical transport. The transport properties of light in a variety of circuit geometries are studied. Emphasis is placed on network geometries, which include barriers formed by the addition of dielectric materials to waveguide channels, bends in waveguide channels, closed loops, and interconnecting branched networks. Results for the transmission and reflection properties of photonic circuit modes are presented as functions of the mode frequencies and the dielectric constants of the materials forming the waveguide channels. A comparison is made of the properties of photonic crystal circuits with those of layered optical systems.

I. INTRODUCTION

There has been considerable recent interest in photonic crystal waveguides.¹⁻¹⁴ These are waveguide structures formed in photonic crystals by the addition of a line of site impurities to the photonic crystal. Electromagnetic waveguide modes then propagate along the line of site impurities. The interest in these structures has been in their use for the efficient transportation of electromagnetic energy and in the channeling of the motion of electromagnetic energy through space.^{1,2} Photonic crystal waveguides are designed to conduct propagating electromagnetic modes along the length of the waveguide material at frequencies that occur in the stop gaps of the photonic crystal. Waveguide modes at stop-gap frequencies of the photonic crystal are found to be very stable against radiative loss from the waveguide channel and tend to efficiently move electromagnetic energy along waveguide channels even in the presence of bends or junctions in the channel.^{1,2,4-6} A recent review of waveguide structures in photonic crystals has been given by Joannopoulos *et al.*,² as well as in an earlier book¹ devoted to the topic of photonic crystals. In some more recent work, we have investigated the existence in nonlinear photonic crystals of static and propagating intrinsic localized modes.^{13,14}

One interest in waveguides has been in forming from them branching waveguide structures in photonic crystals.⁸ We refer to these networks as photonic crystal circuits. They are systems of two or more waveguides that join together to form conducting paths for the transportation of electromagnetic energy in space in a manner analogous to the transportation of electrical current through space in electrical circuits. A very interesting recent work on these types of problems has appeared in Ref. 8, which presents studies of a circuit consisting of two parallel waveguide channels that are linked by a short segment of waveguide. The waveguide channels are formed by removing rods from a two-dimensional photonic crystal, and the modes of the system are determined using techniques of supercell computer simulation.⁸ Similar computer simulations based on supercell methods had earlier

been used by these authors to study bends in photonic crystal waveguides as well as in other seminal studies of photonic crystal waveguides.²

Most theoretical studies of photonic crystal waveguides and their branching networks have been based on supercell computer simulations methods and have focused on systems with waveguide channels formed by removing rows of dielectric rods from photonic crystals. These studies are limited in two ways: First, they are limited in the size of the systems that can be treated by supercell computations, and second, they are limited in the types of waveguide channels that have been treated. In this paper we will present a theory that is not limited by either of these conditions.

In this paper we study the theory of branching structures of photonic waveguides using a method based on Green's functions. The method is not restricted by network size limitations and can be applied to general network geometries in photonic crystals of any dimensionality. In addition, the Green's function method can be easily applied to waveguide channels formed from different dielectric materials or materials that have a number of different interconnecting waveguide channels all formed from different types of dielectric materials. In this approach, Green's functions techniques are applied^{3,9-14} to particular types of photonic crystal waveguides for which the equations describing the propagation of light in the waveguide channels reduce to a set of difference equations. These difference equations are treated using standard methods to obtain analytic closed-form expressions for the propagation characteristics of photonic crystal circuits.

We illustrate the difference equation techniques by applying them to a variety of photonic crystal circuits in two-dimensional photonic crystals. We emphasize, however, that the difference equations can be directly applied to circuits in three-dimensional photonic crystals so that the dimensionality of the circuit network does not restrict the mathematics of the theory. For the two-dimensional photonic crystal a square lattice array of infinitely long dielectric rods is considered.

The rods are of circular cross section with axes parallel to the z axis and form a square lattice with lattice constant a_c in the x - y plane. The waveguide channels of the photonic crystal circuits are formed by replacing rows of rods in the photonic crystal by rods containing impurity dielectric media. Only modes propagating in the x - y plane with electric field E polarized parallel to the z axis are studied. For circuits with input and output waveguide lines, results for the transmission and reflection coefficients in these lines as a function of frequency in the stop band of the photonic crystal are obtained. For circuits with closed loops or circuits that are finite isolated waveguide segments, the resonant mode frequencies and field distributions of the modes bound to these types of structures are obtained.

The problem of photonic crystal circuits is closely related to another important problem in optics: layered optical media. A long straight photonic crystal waveguide exhibits many of the properties of layered systems, e.g., stop- and pass-band, transmission, and reflection characteristics. A dielectric barrier placed in a photonic crystal waveguide exhibits transmission and reflection features similar to dielectric barriers in layered systems. Photonic crystal circuits, however, are higher-dimensional systems than are one-dimensional layered systems, and due to their branching networks exhibit a wider variety of physical phenomena than do layered optical media. A circuit with a number of interconnecting sidebranches shows multiple phase coherence effects due to the multiplicity of paths light can travel. The new phase coherence shows up in the complex reflection and transmission coefficient properties of photonic crystals circuits with input and output channels. An additional feature of photonic crystal circuits is that they, unlike layered media, can close upon themselves (e.g, make a closed-loop circuit), and these structure can bind resonant modes similar to those found in cavity resonators.

The order of this paper will be as follows: In Sec. II, we discuss the network geometry and forms of electromagnetic solutions in photonic crystal circuits. The derivation of the difference equations describing the waveguide modes is presented. This derivation is essentially a generalization of the derivation of the difference equations found in Ref. 13, to treat branching network geometries and waveguide channels containing sections with different types of dielectric material. The remainder of the paper is devoted to obtaining solutions of these equations for particular networks. In Sec. III, a discussion is given of waveguides that are of finite length, terminate at a point in the photonic crystal, contain dielectric barriers, or have channels with bends in space. Explicit analytic expressions are given for the transmission and reflection characteristics of these geometries. In Sec. IV, systems of branched waveguides (branching networks) are treated, and the characteristics of the propagation of electromagnetic waves are determined. In a first case a waveguide junction in which a semi-infinite waveguide is joined at a single site of an infinitely long waveguide is treated. This is next generalized to consider a U-shaped waveguide that joins at two sites onto an infinitely long waveguide. The final two systems studied are one formed from two infinitely long parallel waveguides that are joined together by a short segment and the case of a closed-loop waveguide. The complex behavior in the reflection and transmission coefficients due to phase

coherence and path multiplicity in these networks is discussed. For finite closed-loop systems the bound state resonant modes and their resonant frequencies are determined. In Sec. V, conclusions are given.

II. DIFFERENCE EQUATIONS FOR PHOTONIC CRYSTAL WAVEGUIDES

As in Ref. 13, we consider the E -polarized electromagnetic modes of a two-dimensional photonic crystal formed as a square lattice array of infinitely long, parallel, identical dielectric rods.^{13,15-17} The rods, which are of circular cross section, are characterized by a dielectric constant ϵ and are embedded in vacuum.^{13,15} The periodic dielectric constant of the system as a function of position, $\vec{r}_{||} = x\hat{i} + y\hat{j}$, in the x - y plane is then

$$\epsilon(\vec{r}_{||}) = \begin{cases} \epsilon, & |\vec{r}_{||} - na_c\hat{i} - ma_c\hat{j}| \leq R \text{ for } n \text{ and } m \text{ integers} \\ 1, & \text{otherwise} \end{cases} \quad (1)$$

where a_c is the lattice constant of the square lattice, and $R < a_c$ is the radius of the dielectric rods. The E -polarized electromagnetic modes of the photonic crystal that propagate in the x - y plane are solutions of the matrix eigenvalue equation^{13,15}

$$(\vec{k}_{||} + \vec{G}_{||})^2 e(\vec{k}_{||} | \vec{G}_{||} | \omega) = \frac{\omega^2}{c^2} \sum_{\vec{G}'_{||}} \hat{\epsilon}(\vec{G}_{||} - \vec{G}'_{||}) e(\vec{k}_{||} | \vec{G}'_{||} | \omega). \quad (2)$$

Here the eigenvalue ω^2/c^2 gives the frequency ω of the electromagnetic mode, $\vec{G}_{||}$ is a reciprocal-lattice vector of the square lattice, $\epsilon(\vec{r}_{||}) = \sum_{\vec{G}_{||}} \hat{\epsilon}(\vec{G}_{||}) e^{i\vec{G}_{||} \cdot \vec{r}_{||}}$, and $e(\vec{k}_{||} | \vec{G}_{||} | \omega)$ are related to the electric field, $E(\vec{r}_{||} | \omega)$, of the mode of frequency ω by

$$E(\vec{r}_{||} | \omega) = \sum_{\vec{G}_{||}} e(\vec{k}_{||} | \vec{G}_{||} | \omega) e^{i(\vec{k}_{||} + \vec{G}_{||}) \cdot \vec{r}_{||}}. \quad (3)$$

A waveguide impurity is formed in the system defined in Eq. (1) by adding impurity material to a row of rods along one of the directions of the square lattice.^{13,15} Waveguides of both infinite and finite lengths in the photonic crystal can be made in this way, and we now discuss these two types. Impurity material can be added to an infinite number of rods in a row of rods in the photonic crystal so as to form an infinitely long waveguide. For example, an infinite waveguide is formed when impurity material is added to the sites $\{(nra_c, nsa_c)\}$, where r and s are fixed integers and $n = -\infty, \dots, -2, -1, 0, 1, 2, \dots, \infty$ ranges over the integers. Impurity material can also be added to a finite number of rods in a row of rods of the photonic crystal so as to form a finite-length waveguide segment. For example, such a finite segment is formed for the case in which impurity material is added to the sites $\{(nra_c, nsa_c)\}$, where r and s are fixed integers and $n = 0, 1, 2, \dots, m$ where m is an integer. One can then form a branching system of waveguides (photonic circuits) by piecing together various waveguide segments.

The total dielectric constant of a waveguide segment, $\epsilon_T(\vec{r}_{||})$, is given by $\epsilon_T(\vec{r}_{||}) = \epsilon(\vec{r}_{||}) + \delta\epsilon(\vec{r}_{||})$, where $\delta\epsilon(\vec{r}_{||})$ is the change in the dielectric constant of the photonic crystal upon the addition of impurity dielectric material. For a waveguide segment composed of an array of identical single-site impurities of square cross-sectional area in the x - y plane, $\delta\epsilon(\vec{r}_{||})$ is¹³

$$\delta\epsilon(\vec{r}_{||}) = \begin{cases} \delta\epsilon, & |x - nra_c|, |y - nsa_c| \leq t \text{ for } \{n\} \text{ integers} \\ 0, & \text{otherwise} \end{cases} \quad (4)$$

where r and s are fixed integers, the length of the waveguide segment depends on the range of the consecutive integers $\{n\}$, and $2t$ is the length of a side of one of the single-site impurities. For the impurities we consider $2t \ll R < a_c$. [At this point, we emphasize that $\delta\epsilon$ in Eq. (4) is the value of the dielectric constant of the impurity material minus the dielectric constant of the material forming the pure dielectric rods of the photonic crystal.] We now turn to a discussion of the electric fields associated with such waveguide segments and the photonic circuits formed by piecing them together.

We assume that the electric field of the modes associated with waveguide segments and their branchings is of the form

$$E(\vec{r}_{||}|t) = E^0(\vec{r}_{||}, \omega) \exp(-i\omega t). \quad (5)$$

Using standard techniques,^{3,9-13} the electric field of waveguide segments and their branchings is expressed as an integral equation given by

$$E^0(\vec{r}_{||}, \omega) = \int d^2r'_{||} G(\vec{r}_{||}, \vec{r}'_{||}|\omega) \delta\epsilon(\vec{r}'_{||}) \left(\frac{\omega}{c}\right)^2 E^0(\vec{r}'_{||}, \omega), \quad (6)$$

where $\delta\epsilon(\vec{r}_{||})$ is the change in the photonic crystal dielectric constant due to all of the waveguide segments and their branchings in the photonic crystal. Here $G(\vec{r}_{||}, \vec{r}'_{||}|\omega)$ is the Green's function of the Helmholtz operator for the photonic crystal in Eq. (1), i.e., $\nabla^2 + \epsilon(\vec{r}_{||})(\omega/c)^2$.

As in Ref. 13 we assume that t is small enough so that the electromagnetic field at each square cross-section rod of impurity material is constant over that volume of the impurity material. This assumption allows us to rewrite Eq. (6) for the fields in the rods as a difference equation. For example, consider $\delta\epsilon(\vec{r}_{||})$ as defined in Eq. (4) for a waveguide segment formed from identical single-site impurities. Let the electric field in the rod of impurity material of the waveguide labeled by (nr, ns) in Eq. (4) be denoted by $E_{nr, ns}$, where $E_{nr, ns} = E^0(n(r\hat{i} + s\hat{j})a_c, \omega)$; then we obtain from Eq. (6) for this segment the difference equation

$$E_{nr, ns} = \sum_m B_{nr, ns; mr, ms} \delta\epsilon(m(r\hat{i} + s\hat{j})a_c) E_{mr, ms}. \quad (7)$$

Here

$$B_{nr, ns; mr, ms} = \left(\frac{\omega}{c}\right)^2 \int_{(mr, ms) \text{th impurity}} d^2r_{||} \times G(n(r\hat{i} + s\hat{j})a_c, \vec{r}_{||}|\omega), \quad (8)$$

in the sum in Eq. (7) m runs over the integers denoting the waveguide channel sites, and ω is the frequency of the impurity mode. For our purposes ω will be chosen to be in one of the stop gaps of the photonic crystal described in Eq. (1). From Eqs. (7) and (8) we then have

$$E_{nr, ns} = A \sum_{mr, ms} B_{nr, ns; mr, ms} E_{mr, ms}, \quad (9)$$

where $A = \delta\epsilon$, and again $\delta\epsilon$ is the value of the dielectric constant of the impurity material minus ϵ of the photonic crystal rods. Equation (9) determines the fields in the impurity rods forming the photonic crystal waveguide. As we shall see in the next sections, Eqs. (7) and (9) are easily and naturally generalized to obtain from Eq. (6) a series of interconnecting difference equations describing more general photonic circuits.

Following the discussion in Refs. 11 through 14, the mathematics of our treatment is simplified by restricting the recursion relation in Eq. (9) to consider only same-site and nearest-neighbor site couplings. We do this as the couplings, as seen in Eq. (8), are related to the Green's function $G(\vec{r}_{||}, \vec{r}'_{||}|\omega)$, which decays with increasing $|\vec{r}_{||} - \vec{r}'_{||}|$ for ω in a stop gap of the photonic crystal. For directions of high Miller indices this decay is expected to be large. We refer the reader to Refs. 11 through 14 for a more detailed discussion of this approximation, which has also been used there. The reader will see, however, that the restrictions to same-site and nearest-neighbor site couplings just simplifies the mathematics of our treatment below. Further-neighbor couplings can be included. These only make the mathematics in the following sections a little tedious. With this provision Eq. (9) becomes

$$E_{nr, ns} = \gamma[\alpha(0,0)E_{nr, ns} + \alpha(r,s)(E_{(n+1)r, (n+1)s} + E_{(n-1)r, (n-1)s})]. \quad (10)$$

Here $\alpha(0,0) = B_{0,0;0,0}/(4t^2)$, $\alpha(r,s) = B_{0,0;r,s}/(4t^2)$, where r and s are defined in Eq. (4), and $\gamma = 4t^2 \delta\epsilon$. The electromagnetic mode solutions of Eq. (10) that are bound to the waveguide are obtained by first choosing ω to be a frequency in the stop band of the photonic crystal and computing $\alpha(0,0)$ and $\alpha(r,s)$. Equation (10) can then be solved for $\{E_{nr, ns}\}$ and γ (i.e., $4t^2 \delta\epsilon$) characterizing these modes.

We now turn to a discussion of the evaluation of this theory for a variety of different geometries. In this discussion we present closed-form analytic expressions for the fields of the modes, the mode frequencies, and the transmission and reflection coefficients of a variety of systems that are of interest. We will offer plots illustrating the results from some of these expressions for a particular realization of a two-dimensional photonic crystal.^{9,11} For the particular two-dimensional photonic crystal used in our illustration,^{9,11} the plots presented in the text and those the reader may wish to generate for the other systems considered in this paper can be easily produced on a pocket calculator using the equations in the text and the numerical results for the coefficients $\alpha(r,s)$ given in the Appendix. Finally, we note here that the difference equations studied in this paper are closely related, in the absence of a Kerr nonlinearity, to those studied in Ref. 13. An essential difference in the difference equations studied

here is that they are for branched networks, whereas the difference equations in Ref. 13 were for infinitely long straight waveguide channels.

III. FINITE LENGTH AND SEMI-INFINITE WAVEGUIDES, DIELECTRIC BARRIERS, AND BENDS

A. Finite length

Equation (10) can be used to treat a finite length of waveguide embedded in a photonic crystal. We shall start by considering the simplest case of a single-site impurity and then generalizing this to the study of a finite length segment of single-site impurities.

For a single impurity site^{1,2,9} located at $(nr, ns) = (0, 0)$, we have from Eq. (10)

$$E_{0,0} = \gamma \alpha(0,0) E_{0,0}. \quad (11)$$

Computing $\alpha(0,0)$ for ω in the stop gap of the photonic crystal, we find that

$$\gamma = \alpha(0,0)^{-1} \quad (12)$$

determines the value of $\gamma = 4t^2 \delta\epsilon$ needed to obtain an impurity mode of frequency ω bound to the impurity site material. For a two-site impurity at, for example, sites located at $(0,0)$ and (r,s) , the two equations obtained from Eq. (10) are

$$E_{0,0} = \gamma [\alpha(0,0) E_{0,0} + \alpha(r,s) E_{r,s}] \quad (13)$$

and

$$E_{r,s} = \gamma [\alpha(0,0) E_{r,s} + \alpha(r,s) E_{0,0}]. \quad (14)$$

From $\alpha(0,0)$ and $\alpha(r,s)$ evaluated at the impurity mode frequency ω , we find two solutions for γ :

$$\gamma = [\alpha(0,0) + \alpha(r,s)]^{-1} \quad (15)$$

and

$$\gamma = [\alpha(0,0) - \alpha(r,s)]^{-1}. \quad (16)$$

These solutions give the values of $\gamma = 4t^2 \delta\epsilon$ at which impurity modes are observed at the frequency ω .

The considerations above based on Eq. (10) can be extended to the treatment of a segment of $l+1$ sites, where $l > 1$, located at (ir, is) for $i=0,1,\dots,l$. Proceeding as above for $\alpha(0,0)$ and $\alpha(r,s)$ evaluated at the impurity mode frequency ω , we find that the γ needed to observe impurity modes at ω are obtained from the matrix eigenvalue problem of the tridiagonal matrix defined by

$$E_{0,0} = \gamma [\alpha(0,0) E_{0,0} + \alpha(r,s) E_{r,s}], \quad (17)$$

$$E_{ir,is} = \gamma [\alpha(0,0) E_{ir,is} + \alpha(r,s) (E_{(i-1)r,(i-1)s} + E_{(i+1)r,(i+1)s})], \quad (18)$$

where $i=1,2,\dots,l-1$, and

$$E_{lr,ls} = \gamma [\alpha(0,0) E_{lr,ls} + \alpha(r,s) E_{(l-1)r,(l-1)s}]. \quad (19)$$

The solution of Eqs. (17) through (19) gives

$$\gamma = [\alpha(0,0) + 2\alpha(r,s) \cos k]^{-1}, \quad (20)$$

where $k = \pi N / (l+2)$ for N an integer for the values of γ that are needed to support impurity modes of frequency ω . The fields $\{E_{nr,ns}\}$ are obtained as the eigenvectors for a given eigenvalue $\gamma = 4t^2 \delta\epsilon$. In general, we see that a finite isolated waveguide of length l binds to it a series of resonant modes. The modes occur at a discrete set of frequencies and wave numbers that are the solution of Eqs. (12) or (15) and (16) or (20) for fixed $\gamma = 4t^2 \delta\epsilon$. It is interesting to see that by tuning $\gamma = 4t^2 \delta\epsilon$ we can adjust the series of resonant modes of the finite length of waveguide.

The evaluation of the structures described by Eqs. (12), (15), (16), and (20) is quite simple. Once the $\alpha(r,s)$ have been evaluated at a frequency in the stop band for a given photonic crystal, the solution for the change in dielectric constant $\delta\epsilon$ to have a resonance mode at this frequency is easily obtained from Eqs. (12), (15), (16), and (20). We have discussed this evaluation in detail in the case of impurity clusters of highly symmetric geometry in Ref. 9. This discussion can be directly taken over to the new types of impurities considered above. To assist the reader, however, we give a discussion in the Appendix of the evaluation of the impurity equations given above.

B. Terminated waveguides, waveguides containing barriers, and bends

In Refs. 11–14 we have treated waveguides with infinitely long uniform waveguide channels formed from both linear and Kerr nonlinear impurity dielectric media. In the following subsection, we shall extend the ideas in Refs. 11–14 to consider the properties of new varieties of waveguides, which include semi-infinite waveguides terminated in the photonic crystal and infinitely long waveguides containing dielectric barriers. We restrict our considerations to linear impurity dielectric media.

A semi-infinite waveguide that terminates in the photonic crystal is a waveguide with a long straight channel that ends at some point in the photonic crystal. This system can be described from Eq. (6) in our model by the following set of difference equations:

$$E_{0,0} = \gamma [\alpha(0,0) E_{0,0} + \alpha(r,s) E_{r,s}], \quad (21)$$

$$E_{ir,is} = \gamma [\alpha(0,0) E_{ir,is} + \alpha(r,s) (E_{(i-1)r,(i-1)s} + E_{(i+1)r,(i+1)s})], \quad (22)$$

where $i=1,2,3,\dots$. The waveguide channel terminates at the site $(0,0)$ and comes in linearly in space to $(0,0)$ from the (r,s) direction.

To solve the system of equations in Eqs. (21) and (22) we compute $\alpha(0,0)$ and $\alpha(r,s)$ at the impurity frequency ω and assume a solution of Eqs. (21) and (22) of the form

$$E_{lr,ls} = e^{ilk} + b e^{-ilk} \quad (23)$$

for $l=0,1,2,\dots$, where k is the wave number that gives the phase change in $E_{lr,ls}$ from site to site along the waveguide channel. Substituting in Eqs. (21) and (22) we find

$$\gamma = [\alpha(0,0) + 2\alpha(r,s) \cos k]^{-1} \quad (24)$$

and $b = -e^{-2ik}$. The waveguide modes are just standing wave modes that are trapped in the waveguide channel be-

cause their frequencies are in the stop gaps of the photonic crystal; each mode is formed from two oppositely moving waves that are phase shifted by b . For a fixed dielectric difference $\delta\epsilon$ and a fixed value of t , the solution of Eq. (24) for fixed $\gamma = 4t^2\delta\epsilon$ gives the frequencies and wave numbers k of the mode solutions. In the Appendix results for $\alpha(r,s)$ are given for a particular realization of a photonic crystal. These can be used to map out the solutions of Eq. (24).

Next we consider an infinitely long, straight waveguide that contains a dielectric barrier. A dielectric barrier is created in the waveguide by changing the dielectric impurity material in $2n+1$ consecutive sites in the channel of the dielectric waveguide to a new type of impurity material. (This is the analogy in the optics of layered systems to considering normal incidence of light on a dielectric slab.) The difference equations describing this system are from Eq. (6) in our model,

$$E_{lr,ls} = \gamma_0[\alpha(0,0)E_{lr,ls} + \alpha(r,s)(E_{(l+1)r,(l+1)s} + E_{(l-1)r,(l-1)s})], \quad (25)$$

where $l = \pm(n+2), \pm(n+3), \dots$,

$$E_{ir,is} = \gamma_1[\alpha(0,0)E_{ir,is} + \alpha(r,s)(E_{(i+1)r,(i+1)s} + E_{(i-1)r,(i-1)s})], \quad (26)$$

where $i = 0, \pm 1, \dots, \pm(n-1)$,

$$E_{\pm nr, \pm ns} = \gamma_1[\alpha(0,0)E_{\pm nr, \pm ns} + \alpha(r,s)E_{\pm(n-1)r, \pm(n-1)s}] + \gamma_0\alpha(r,s)E_{\pm(n+1)r, \pm(n+1)s}, \quad (27)$$

$$E_{\pm(n+1)r, \pm(n+1)s} = \gamma_0[\alpha(0,0)E_{\pm(n+1)r, \pm(n+1)s} + \alpha(r,s)E_{\pm(n+2)r, \pm(n+2)s}] + \gamma_1\alpha(r,s)E_{\pm nr, \pm ns}. \quad (28)$$

In the above equations γ_0 and γ_1 reflect the difference in the impurity dielectric constant of the material forming the waveguide channel and the new material inserted in the waveguide channel forming the barrier in the waveguide channel.

In solving the difference equations in Eqs. (25)–(28) we first choose the frequency ω of the modes of the waveguide with the barrier system. The frequency is chosen to be in the stop band of the photonic crystal. The constants $\alpha(0,0)$ and $\alpha(r,s)$ are evaluated for this ω and the resulting difference equations are solved for the $\{E_{mr,ms}\}$, γ_0 , and γ_1 using standard techniques. Note that the values of both γ_0 and γ_1 needed to support a mode of frequency ω are restricted and must be determined from the set of difference equations.

Let us assume a solution of Eqs. (25)–(28) of the form

$$E_{lr,ls} = fe^{-ikl} + ae^{ikl}, \quad (29)$$

where $l = (n+1), (n+2), \dots$,

$$E_{lr,ls} = be^{-iql} + ce^{iql}, \quad (30)$$

where $l = 0, \pm 1, \pm 2, \dots, \pm n$,

$$E_{lr,ls} = de^{-ikl} + e_0e^{ikl}, \quad (31)$$

where $l = -(n+1), -(n+2), \dots$. Substituting Eqs. (29) and (31) into Eq. (25) we find that

$$\gamma_0 = [\alpha(0,0) + 2\alpha(r,s)\cos k]^{-1}, \quad (32)$$

and substituting Eq. (30) in Eq. (26) we find that

$$\gamma_1 = [\alpha(0,0) + 2\alpha(r,s)\cos q]^{-1}. \quad (33)$$

Equations (32) and (33) give the possible dielectric constants, respectively, of the impurity materials in the waveguide channel and the barrier for the system to support a propagating waveguide mode of frequency ω , with wave number k in the waveguide channel outside of the barrier, and wave number q in the waveguide channel inside of the barrier material. In the following, it is assumed that $k \neq q$ so that $\gamma_0 \neq \gamma_1$. Using Eqs. (27) and (28) to match the boundary conditions at the edge of the barrier, we obtain

$$\begin{vmatrix} f \\ a \end{vmatrix} = \begin{vmatrix} b_1 & b_2 \\ b_2^* & b_1^* \end{vmatrix} \begin{vmatrix} d \\ e_0 \end{vmatrix}, \quad (34)$$

where

$$b_1 = -e^{2ik(n+1)}(e^{-2iqn}[1 - e^{-i(k+q)}]^2 - e^{2iqn}[1 - e^{-i(k-q)}]^2)/(4 \sin k \sin q) \quad (35)$$

and

$$b_2 = -(e^{-2iqn}[1 - e^{-i(k+q)}] \times [1 - e^{i(k-q)}] - \text{c.c.})/(4 \sin k \sin q). \quad (36)$$

Equation (34) represents a transform between the states in Eqs. (29) and (31) on opposite sides of the barrier. This transform conserves the total energy flux along the length of the waveguide. As an example, to treat a scattering problem involving a wave incident on the barrier from the right we can evaluate Eq. (34) for $d=1$ and $e_0=0$. This gives the incident wave amplitude, $f=b_1$, and the reflected wave amplitude, $a=b_2^*$, on the right of the barrier for there to be a unit transmitted wave on the left of the barrier. Specifically, for a unit transmitted flux on the left of the barrier the relative intensity of the incident flux on the right of the barrier is $|f|^2 = \{(1 - \cos k \cos q)^2 + \sin^2 k \sin^2 q - [\cos q - \cos k]^2 \cos[(4n+2)q]\}/[2 \sin^2 q \sin^2 k]$, and the relative intensity of the reflected flux on the right of the barrier is $|a|^2 = \{(1 - \cos k \cos q)^2 - \sin^2 k \sin^2 q - [\cos q - \cos k]^2 \cos[(4n+2)q]\}/[2 \sin^2 k \sin^2 q]$. The transmission coefficient, defined as the ratio of the transmitted to incident power flux is then given by

$$T = \frac{2 \sin^2 q \sin^2 k}{(1 - \cos k \cos q)^2 + \sin^2 k \sin^2 q - (\cos q - \cos k)^2 \cos((4n+2)q)}, \quad (37)$$

and the reflection coefficient is $R = 1 - T$.

To illustrate the results for the transmission of electromagnetic waveguide modes through the dielectric barrier, we have plotted in Fig. 1 results for the barrier transmission coefficient, Eq. (37), versus the frequency ω in the stop band of a square lattice photonic crystal. These results are obtained from the evaluation of Eqs. (32), (33), and (37). The photonic crystal we study is an array of cylindrical dielectric rods of dielectric constant $\epsilon = 9$ and radius $R = 0.37796a_c$, where a_c is the lattice constant of the square lattice. The dielectric rods are surrounded by vacuum. This particular photonic crystal has a stop band at $0.425 < \omega a_c / 2\pi c < 0.455$. The waveguide channel is taken to be in the [10] direction and is formed from impurity materials with $t = 0.01a_c$. The impurities forming the waveguide channel are taken to have a nearest-neighbor separation of a lattice constant so that in Eqs. (32) and (33) $\alpha(r,s) = \alpha(1,0)$, and for the results presented in Fig. 1 we have taken $n = 10$. We refer the reader to the Appendix for a more detailed discussion of the generation of Fig. 1 from the equations in the text. In Fig. 1 and the remaining figures presented in the text, we will only show results obtained from the evaluation of the equations generated in the body of the text. We will indicate in the text which equations are used to generate the figures but will refer the interested reader to the Appendix for a detailed discussion of the particulars as to the generation of the figures from the text materials.

The plots in Fig. 1 are obtained by fixing the values of γ_0 and γ_1 and varying the waveguide mode frequency over the stop gap of the photonic crystal. To obtain plots that sample as much of the parameter space available for study in this model as possible, we have chosen values of γ_0 and γ_1 for these plots, which give a diverse selection of values of q and k at the mid-stop-band frequency. Specifically, if we denote the values of q and k at the mid-stop-band frequency, $\omega a_c / 2\pi c = 0.440$, by q_c and k_c , we present plots for the pairs $(q_c, k_c) = (\pi/2, \pi)$, $(\pi/2, \pi/100)$, $(\pi/10, \pi/2)$, $(\pi/10, \pi/4)$, $(\pi, \pi/4)$, and $(\pi, \pi/2)$. From Eq. (A3) in the Appendix, we see that these correspond to $\gamma_0/\gamma_1 = 1.20, 0.86, 1.16, 1.04, 0.74,$ and 0.83 , respectively. The values of (q_c, k_c) we treat then sample regions in which the ratio of the wave vectors in the barrier medium and in the waveguide channel medium are large or small for q_c taken at the bottom of the band ($q_c \approx 0$), at the center of the band ($q_c = \pi/2$), and at the top of the band ($q_c = \pi$). In general, the transmission coefficients in Fig. 1 as functions of the frequency of the modes are found to exhibit a roughly periodic series of interference maxima and minima related to the interference of the transmitted and reflected waves at the barrier surfaces. This is the type of behavior observed in barrier reflection in layered optical systems. It is interesting to note that the period in frequency of the maxima and minima of the transmission coefficient is relatively insensitive to the values of (q_c, k_c) . In addition, the transmission coefficients are seen to

be nonzero over different frequency intervals of the stop band. This is due to the different dispersion characteristics of the waveguide channels for different values of γ_0 and γ_1 .

The barrier region in which $l = -n, -(n+1), \dots, -1, 0, 1, \dots, n-1, n$ does not have to be made from material that conducts electromagnetic waves [i.e., has a plane-wave waveguide mode solution of the form in Eq. (30)] for the frequency ω . If we analytically continue Eqs. (30), (33), (35), and (36) by replacing q by $-iq$, then the solution in the barrier becomes from Eq. (30)

$$E_{lr,ls} = b e^{-q^l} + c e^{q^l}, \quad (38)$$

which is a nonpropagating form. From Eq. (33) we find that γ_1 supporting these modes is given by

$$\gamma_1 = [\alpha(0,0) + 2\alpha(r,s) \cosh q]^{-1}, \quad (39)$$

and a new Eq. (34) relating f, a to d, e_0 for this system is found by similarly replacing q by $-iq$. If we perform an analytical continuation by replacing q by $-iq + \pi$, then the nonpropagating solutions in the barrier becomes from Eq. (30)

$$E_{lr,ls} = (-1)^l [b e^{-q^l} + c e^{q^l}], \quad (40)$$

where γ_1 supporting these modes is given by

$$\gamma_1 = [\alpha(0,0) - 2\alpha(r,s) \cosh q]^{-1}, \quad (41)$$

and a new Eq. (34) relating a, f to d, e_0 for this case is found by similarly replacing q by $-iq + \pi$. Equations (33), (39), and (41) then account for all possible values $-\infty \leq \gamma_1 \leq \infty$ of interest in the barrier problem.

Another geometry of interest is that of an infinitely long waveguide with a bend. We shall treat the case of a right-angle bend in a square lattice photonic crystal with one part of the waveguide on the negative x axis and the other part on the positive y axis. From Eq. (6), in the small- t approximation, we obtain a set of difference equations given below. It is interesting to note here, however, that if we only consider the case of such a waveguide with nearest-neighbor interactions, there is no difference in the difference equations for the cases of a waveguide with or without a bend. Differences arise, however, when further than nearest-neighbor interactions occur in the system. Consequently, we shall treat a system with nearest- and next-nearest-neighbor interactions for a right-angle waveguide. The waveguide channel we consider is formed of a single type of dielectric impurity material.

Consider the geometry in Fig. 2(a). The difference equations defining the waveguide are from Eq. (6), using the notation of Eq. (10),

$$E_{lr,0} = \gamma_0 [\alpha(0,0) E_{lr,0} + \alpha(r,0) (E_{(l+1)r,0} + E_{(l-1)r,0})], \quad (42)$$

where $l = -2, -3, -4, \dots$,

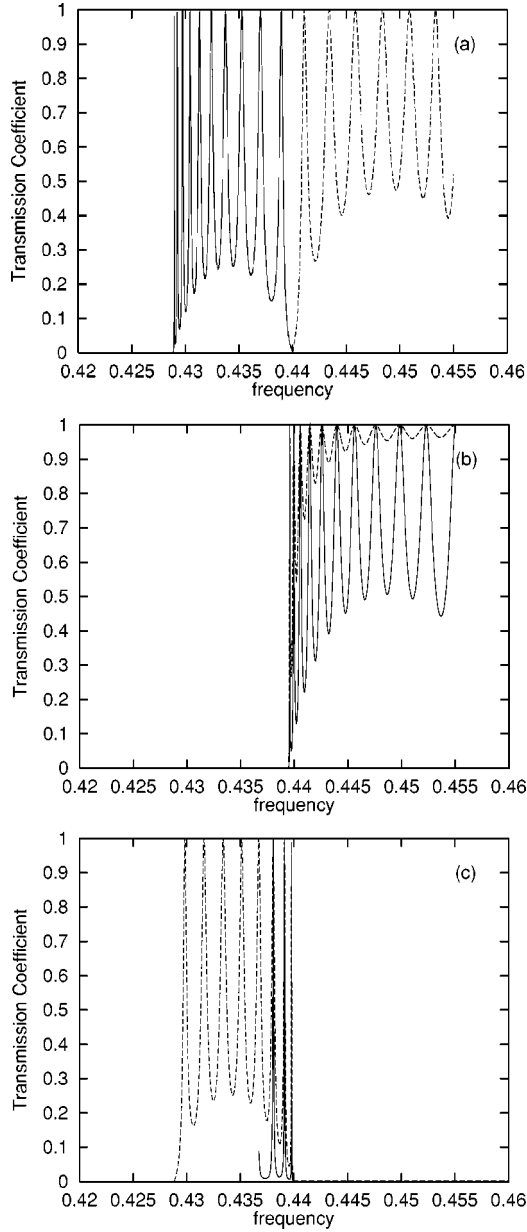


FIG. 1. Results for the barrier problem. Plots for the transmission coefficient versus frequency in units of $\omega a_c/2\pi c$ are shown for $(q_c, k_c) =$ (a) $(\pi/2, \pi)$ (solid) and $(\pi/2, \pi/100)$ (dashed), (b) $(\pi/10, \pi/2)$ (solid) and $(\pi/10, \pi/4)$ (dashed), (c) $(\pi, \pi/4)$ (solid) and $(\pi, \pi/2)$ (dashed).

$$E_{0,lr} = \gamma_0 [\alpha(0,0)E_{0,lr} + \alpha(0,r)(E_{0,(l+1)r} + E_{0,(l-1)r})], \quad (43)$$

where $l = 2, 3, 4, \dots$,

$$E_{-r,0} = \gamma_0 [\alpha(0,0)E_{-r,0} + \alpha(r,0)(E_{-2r,0} + E_{0,0}) + \alpha(r,r)E_{0,r}], \quad (44)$$

$$E_{0,0} = \gamma_0 [\alpha(0,0)E_{0,0} + \alpha(r,0)E_{-r,0} + \alpha(0,r)E_{0,r}], \quad (45)$$

and

$$E_{0,r} = \gamma_0 [\alpha(0,0)E_{0,r} + \alpha(r,0)(E_{0,0} + E_{0,2r}) + \alpha(r,r)E_{-r,0}]. \quad (46)$$

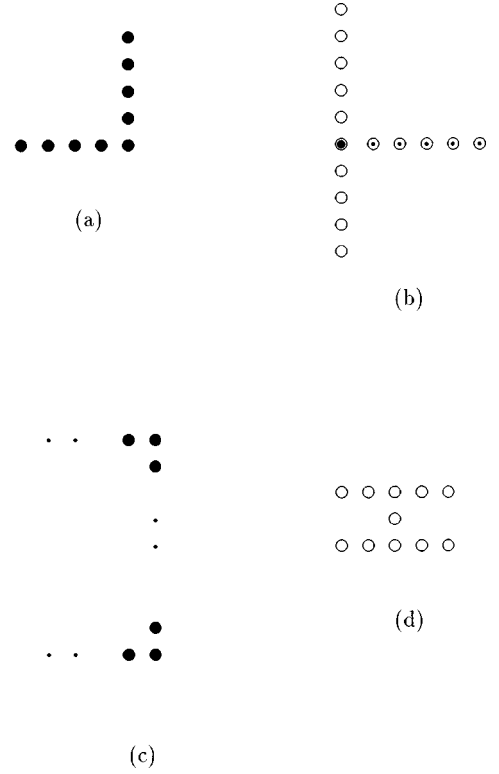


FIG. 2. Schematic drawings of waveguide channels of photonic crystal circuits. A representation is given in the x - y plane of a two-dimensional photonic crystal formed on a square lattice, i.e., that defined in Eq. (1). In this representation of the waveguide circuits only the rods of the waveguide channel are shown and the remaining rods of the square lattice photonic crystal that are not part of the waveguide channel are not shown. The x axis is horizontal and the y axis is vertical. The nearest-neighbor separation of the rods forming the waveguide channels in the x and y directions are integer multiples of the photonic crystal lattice constant, i.e., see Eq. (4). In these drawings different circles represent rods containing different types of impurity materials. (a) The waveguide with a right angle bend: In this plot the field at the center of the right-angle bend is labeled $E_{0,0}$, and Eq. (42) relates the fields in the horizontal row of rods and Eq. (43) relates the fields in the vertical row of rods. (b) The waveguide junction: The field $E_{0,0}$ is at the connection of the two channels (the circle with the large inside circle), and Eq. (55) relates the fields in the horizontal row of rods and Eq. (56) relates the fields in the vertical row of rods. (c) The infinite waveguide with a U-shaped attachment: The field in the site at the lower left corner of the rectangle is $E_{0,0}$, and Eqs. (83) and (85) relate the fields in the lower and upper horizontal row of solid sites, Eq. (80) relates the fields in the vertical row of open circle sites, and Eq. (84) relates the fields in the vertical row of solid sites. (d) Two infinite parallel waveguide with a single short joint between them: In this figure, the fields in the lower horizontal row of sites are related by Eq. (102), the fields in the upper horizontal row of sites are related by Eq. (103), and the field in the join site between the two waveguide channels is given by Eq. (106).-

Here by symmetry $\alpha(r,0) = \alpha(0,r)$, and the impurity dielectric material on the sites $(0,lr)$ for $l = 0, 1, 2, 3, \dots$ and $(lr,0)$ for $l = -1, -2, -3, \dots$ is characterized by γ_0 .

We look for a solution of this set of equations of the form

$$E_{lr,0} = ae^{ikl} + be^{-ikl}, \quad (47)$$

where $l = -1, -2, \dots$,

$$E_{0,lr} = ce^{ikl} + de^{-ikl}, \quad (48)$$

where $l = 1, 2, \dots$, and

$$E_{0,0} = s. \quad (49)$$

Substituting Eqs. (47) and (48) into Eqs. (42) and (43), we find that $\gamma_0 = [\alpha(0,0) + 2\alpha(r,0)\cos k]^{-1}$. This gives the value of γ_0 needed to observe a waveguide mode of frequency ω and wave number k , where $\alpha(0,0)$ and $\alpha(r,0)$ are evaluated at ω . Substituting Eqs. (47)–(49) into Eqs. (44)–(46) allows us to relate the coefficients a, b to c, d . After a little algebra, we find that the solution forms before and after the bend can be related by

$$\begin{vmatrix} a \\ b \end{vmatrix} = \begin{vmatrix} a_{11} & a_{12} \\ a_{21} & a_{22} \end{vmatrix} \begin{vmatrix} c \\ d \end{vmatrix}, \quad (50)$$

where

$$a_{11} = \frac{\left(2\frac{\alpha(r,r)}{\alpha(r,0)}\cos k + 1\right)^2 e^{2ik} - e^{-2ik}}{2i\sin 2k\left(2\frac{\alpha(r,r)}{\alpha(r,0)}\cos k + 1\right)}, \quad (51)$$

$$a_{12} = \frac{\left(2\frac{\alpha(r,r)}{\alpha(r,0)}\cos k + 1\right)^2 - 1}{2i\sin 2k\left(2\frac{\alpha(r,r)}{\alpha(r,0)}\cos k + 1\right)}, \quad (52)$$

$$a_{21} = a_{12}^*, \quad (53)$$

and

$$a_{22} = a_{11}^*. \quad (54)$$

The matrix equation in Eq. (50) is such that the net power transfer through the bend is conserved along the waveguide, and in the limit that $\alpha(r,r) = 0$ Eq. (50), as expected, yields $a = c$ and $b = d$. Evaluating Eq. (50) for the case $c = 1$ and $d = 0$ gives the amplitudes of the incident wave, $a = a_{11}$, and the reflected wave, $b = a_{12}^*$, for a unit amplitude wave to be transmitted through the bend. It is readily seen that in this case $|a|^2 - |b|^2 = 1$ where

$$\begin{aligned} |a|^2 = & \left\{ \left[\left(2\frac{\alpha(r,r)}{\alpha(r,0)}\cos k + 1\right)^2 - 1 \right]^2 \right. \\ & \left. + 4\sin^2 2k \left(2\frac{\alpha(r,r)}{\alpha(r,0)}\cos k + 1\right)^2 \right\} \\ & \left/ \left[4\sin^2 2k \left(2\frac{\alpha(r,r)}{\alpha(r,0)}\cos k + 1\right)^2 \right] \right. \end{aligned}$$

and

$$\begin{aligned} |b|^2 = & \left[\left(2\frac{\alpha(r,r)}{\alpha(r,0)}\cos k + 1\right)^2 \right. \\ & \left. - 1 \right]^2 \left/ \left[4\sin^2 2k \left(2\frac{\alpha(r,r)}{\alpha(r,0)}\cos k + 1\right)^2 \right] \right. \end{aligned}$$

are the incident and reflected power flux giving rise to a unit transmitted power flux through the bend and that energy is conserved along the waveguide.

IV. BRANCHED WAVEGUIDES AND CIRCUITS

One can make a branched waveguide by attaching a semi-infinite waveguide at a site of an infinite waveguide. [See Fig. 2(b).] We shall assume that the channels of these two waveguides are of different types of impurity materials and the point of attachment is made of a third type of impurity material.

The difference equations describing such a branched waveguide are, from Eq. (6) using the notation of Eq. (10):

$$E_{lr,0} = \gamma_1[\alpha(0,0)E_{lr,0} + \alpha(r,0)(E_{(l-1)r,0} + E_{(l+1)r,0})], \quad (55)$$

where $l = 2, 3, 4, \dots$,

$$E_{0,lr} = \gamma_0[\alpha(0,0)E_{0,lr} + \alpha(r,0)(E_{0,(l-1)r} + E_{0,(l+1)r})], \quad (56)$$

where $l = \pm 2, \pm 3, \pm 4, \dots$,

$$\begin{aligned} E_{0,0} = & \gamma_2\alpha(0,0)E_{0,0} + \gamma_0\alpha(r,0)(E_{0,r} + E_{0,-r}) \\ & + \gamma_1\alpha(r,0)E_{r,0}, \end{aligned} \quad (57)$$

$$E_{0,\pm r} = \gamma_0[\alpha(0,0)E_{0,\pm r} + \alpha(r,0)E_{0,\pm 2r}] + \gamma_2\alpha(r,0)E_{0,0}, \quad (58)$$

and

$$E_{r,0} = \gamma_1[\alpha(0,0)E_{r,0} + \alpha(r,0)E_{2r,0}] + \gamma_2\alpha(r,0)E_{0,0}. \quad (59)$$

We assume a solution of these equations of the form

$$E_{0,lr} = ae^{-ikl} + be^{ikl} \quad (60)$$

for $l = 1, 2, 3, \dots$,

$$E_{0,lr} = ce^{-ikl} + de^{ikl} \quad (61)$$

for $l = -1, -2, -3, \dots$,

$$E_{lr,0} = e_0e^{-iql} + f_0e^{iql} \quad (62)$$

for $l = 1, 2, 3, \dots$, and

$$E_{0,0} = h. \quad (63)$$

Substituting Eqs. (60), (61), and (62) in Eqs. (55) and (56), we find that

$$\gamma_0 = [\alpha(0,0) + 2\alpha(r,0)\cos k]^{-1} \quad (64)$$

and

$$\gamma_1 = [\alpha(0,0) + 2\alpha(r,0)\cos q]^{-1}, \quad (65)$$

which give the impurity dielectric constants in terms of the mode frequency ω and k and q wave numbers in the different branches of the waveguide junction for propagating waveguide modes to exist at frequency ω . The three boundary condition equations in Eq. (57)–(59) then give the matrix equations

$$\begin{pmatrix} e^{-ik} & e^{ik} & e^{ik} & e^{-ik} & \frac{\gamma_1}{\gamma_0} e^{-iq} & \frac{\gamma_1}{\gamma_0} e^{iq} & \frac{\gamma_2 \alpha(0,0) - 1}{\gamma_0 \alpha(r,0)} \\ 1 & 1 & 0 & 0 & 0 & 0 & -\frac{\gamma_2}{\gamma_0} \\ 0 & 0 & 1 & 1 & 0 & 0 & -\frac{\gamma_2}{\gamma_0} \\ 0 & 0 & 0 & 0 & 1 & 1 & -\frac{\gamma_2}{\gamma_1} \end{pmatrix} \begin{pmatrix} a \\ b \\ c \\ d \\ e_0 \\ f \\ h \end{pmatrix} = 0. \quad (66)$$

The solution of the scattering problem for a wave of unit amplitude incident on the branch from $(0, -\infty)$ is obtained by solving Eq. (66) for the case in which $a=0$, $e_0=0$, and $d=1$.

The equations in Eq. (66) can be rewritten as

$$\begin{pmatrix} a_{11} & a_{12} & a_{13} \\ a_{21} & a_{22} & a_{23} \\ a_{31} & a_{32} & a_{33} \end{pmatrix} \begin{pmatrix} a \\ d \\ e_0 \end{pmatrix} = \begin{pmatrix} b \\ c \\ f \end{pmatrix}. \quad (67)$$

Here

$$a_{11} = d_0^{-1} \left(2 \cos k + e^{iq} + \frac{\gamma_2 \alpha(0,0) - 1}{\gamma_2 \alpha(r,0)} \right), \quad (68)$$

$$a_{22} = d_0^{-1} \left(2 \cos k + e^{iq} + \frac{\gamma_2 \alpha(0,0) - 1}{\gamma_2 \alpha(r,0)} \right), \quad (69)$$

$$a_{33} = d_0^{-1} \left(2e^{ik} + e^{-iq} + \frac{\gamma_2 \alpha(0,0) - 1}{\gamma_0 \alpha(r,0)} \right), \quad (70)$$

$$a_{12} = -d_0^{-1} 2i \sin k, \quad (71)$$

$$a_{21} = a_{12}, \quad (72)$$

$$a_{13} = -d_0^{-1} \frac{\gamma_1}{\gamma_0} 2i \sin q, \quad (73)$$

$$a_{31} = -d_0^{-1} 2i \frac{\gamma_0}{\gamma_1} \sin k, \quad (74)$$

$$a_{23} = -d_0^{-1} \frac{\gamma_1}{\gamma_0} 2i \sin q, \quad (75)$$

$$a_{32} = -d_0^{-1} 2i \frac{\gamma_0}{\gamma_1} \sin k, \quad (76)$$

and

$$d_0 = -2e^{ik} - e^{iq} - \frac{\gamma_2 \alpha(0,0) - 1}{\gamma_2 \alpha(r,0)}. \quad (77)$$

Equation (67) then expresses the amplitudes of the waves leaving the vertex (b, c, f) in terms of the waves traveling towards the vertex (a, d, e_0) .

An interesting limiting case is the case in which $q=k$, $\gamma_0 = \gamma_1 = \gamma_2 = \gamma = [\alpha(0,0) + 2\alpha(r,0)\cos k]^{-1}$. In this limit

$a_{11} = a_{22} = a_{33} = -e^{ik}/(\cos k + 3i \sin k)$ and $a_{12} = a_{21} = a_{13} = a_{31} = a_{23} = a_{32} = 2i \sin k/(\cos k + 3i \sin k)$. Sending, in this limit, a unit amplitude flux (e.g., $d=1$, $a=0$, and $e_0=0$) into the junction then from Eq. (67) gives $b=f=2i \sin k/(\cos k + 3i \sin k)$, $c = -e^{ik}/(\cos k + 3i \sin k)$ for the amplitudes of the flux flows away from the junction. We see explicitly that $|d|^2 = |b|^2 + |c|^2 + |f|^2$, where $|b|^2 = |f|^2 = 4 \sin^2 k/(\cos^2 k + 9 \sin^2 k)$ and $|c|^2 = 1/(\cos^2 k + 9 \sin^2 k)$ are the power transmitted and reflected from the junction for a unit incident flux, and consequently flux is conserved at the junction. Defining the reflection and transmission coefficients as the ratios of the reflected and transmitted flux, respectively, to the incident flux, we find for the reflection coefficient

$$R = \frac{1}{\cos^2 k + 9 \sin^2 k} \quad (78)$$

and for the transmission coefficients in each of the two branches leaving the vertex

$$T = \frac{4 \sin^2 k}{\cos^2 k + 9 \sin^2 k}. \quad (79)$$

In Fig. 3 we present plots of T in Eq. (79) versus ω for the branched junction in which all of the waveguide channels are formed from the same material. The plots are made for the photonic crystal studied in Fig. 1 and for a set of waveguide channels in which the impurities forming the channels have a

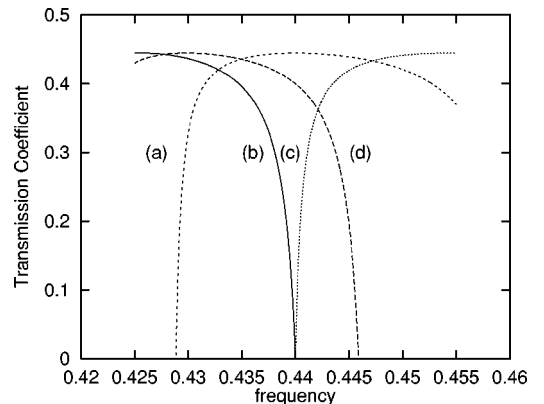


FIG. 3. Results for the junction problem. Plots for the transmission coefficient versus frequency in units of $\omega a_c/2\pi c$ are shown for $k_c =$ (a) $\pi/2$, (b) π , (c) $\pi/100$, (d) $3\pi/4$.

nearest-neighbor separation of a lattice constant. In this photonic crystal $\epsilon=9$, $R=0.37796a_c$, and in the waveguide channel $t=0.01a_c$. Curves are generated from Eq. (79) in conjunction with the dispersion relation $\gamma=[\alpha(0,0)+2\alpha(1,0)]^{-1}$, and are presented as a function of mode frequency for a variety of fixed values of γ . The γ studied are chosen so that the value of k , which we denote as k_c , for the midband frequency $\omega a_c/2\pi c=0.440$ assume a set of representative values $k_c=\pi, 3\pi/4, \pi/2$, and $\pi/100$ corresponding, respectively, to $\gamma=0.342, 0.323, 0.284$, and 0.243 . The reader is again referred to the Appendix for a more detailed account of the treatment of Eq. (79) and the dispersion relation in the generation of the plots in Fig. 3.

In Fig. 3 the transmission coefficients for different values of γ are seen to be nonzero over different regions of the stop band. This is due to the different propagation characteristics of waveguide channels with different γ . In general, the transmission coefficient is fairly constant over the range of frequencies for which it exists. However, the results for all four cases considered display regions of frequencies over which the transmission coefficient rapidly goes to zero. Consequently, in these regions small changes in the incident wave frequency can be used to open and shut the transmission of energy through the junction. All of the systems exhibit a frequency for which the transmission through the junction is a maximum so that by tuning the frequency of the mode one can optimize the transmission of energy through the junction.

Following our discussion of the waveguide with a barrier, we can choose the γ_1 material so as to have nonpropagating (non-plane-wave) waveguide mode solutions. This is done by replacing q by $-iq$ in Eqs. (62), (65), and (68)–(77) so that in this case $\gamma_1=[\alpha(0,0)+2\alpha(r,0)\cosh q]^{-1}$. Alternatively, q can be replaced by $-iq+\pi$ in Eqs. (62), (65), and (68)–(77) so that $\gamma_1=[\alpha(0,0)-2\alpha(r,0)\cosh q]^{-1}$. These two cases along with the $\gamma_1=[\alpha(0,0)+2\alpha(r,0)\cos q]^{-1}$ case of Eq. (65) exhaust the possible values of $-\infty\leq\gamma_1\leq\infty$ in this sidebranch.

Once branching structures can be treated, circuits similar to those involved in the transport of electricity can now be formed for the conduction of photons. As an example of the use of branchings to form a simple photonic circuit, we now treat a waveguide that contains a closed loop. [See Fig. 2(c).]

Consider an infinitely long straight waveguide in a square lattice photonic crystal with the impurity sites of the waveguide channel labeled by $(0,mr)$, where m ranges over the integers. The waveguide is formed of only one type of impurity material. Now attach to the waveguide channel at the $(0,0)$ and $(0,(n+1)r)$ sites for $n>1$ a U-shaped channel of impurities. The impurity material forming the channel of the U can be different from the impurity material forming the channel of the infinitely long waveguide channel. Let us use the above formulation to compute the transmission and reflection characteristics of a waveguide mode incident on the U channel from $(0,-\infty)$.

The set of difference equations that describe this branching geometry consists of ten separate equations. The equations associated with the infinitely long straight waveguide channel are given by the channel equation

$$E_{0,lr}=\gamma_0[\alpha(0,0)E_{0,lr}+\alpha(r,0)(E_{0,(l+1)r}+E_{0,(l-1)r})] \quad (80)$$

where $l\neq 0$ or $n+1$ otherwise ranges over the integers, and two equations connecting the channel to the U-shaped channel

$$E_{0,0}=\gamma_0[\alpha(0,0)E_{0,0}+\alpha(r,0)(E_{0,r}+E_{0,-r})]+\gamma_1\alpha(r,0)E_{r,0}, \quad (81)$$

and

$$E_{0,(n+1)r}=\gamma_0[\alpha(0,0)E_{0,(n+1)r}+\alpha(r,0)(E_{0,(n+2)r}+E_{0,nr})]+\gamma_1\alpha(r,0)E_{r,(n+1)r}. \quad (82)$$

There are seven equations that describe the U-shaped channel. These are

$$E_{lr,0}=\gamma_1[\alpha(0,0)E_{lr,0}+\alpha(r,0)(E_{(l+1)r,0}+E_{(l-1)r,0})], \quad (83)$$

where $l=2,3,\dots,l_0-1$,

$$E_{l_0r,lr}=\gamma_1[\alpha(0,0)E_{l_0r,lr}+\alpha(r,0)(E_{l_0r,(l+1)r}+E_{l_0r,(l-1)r})], \quad (84)$$

where $l=1,2,3,\dots,n$,

$$E_{lr,(n+1)r}=\gamma_1[\alpha(0,0)E_{lr,(n+1)r}+\alpha(r,0)(E_{(l+1)r,(n+1)r}+E_{(l-1)r,(n+1)r})], \quad (85)$$

where $l=2,3,\dots,l_0-1$,

$$E_{l_0r,0}=\gamma_1[\alpha(0,0)E_{l_0r,0}+\alpha(r,0)(E_{l_0r,r}+E_{(l_0-1)r,0})], \quad (86)$$

$$E_{l_0r,(n+1)r}=\gamma_1[\alpha(0,0)E_{l_0r,(n+1)r}+\alpha(r,0)(E_{l_0r,nr}+E_{(l_0-1)r,(n+1)r})], \quad (87)$$

$$E_{r,0}=\gamma_1[\alpha(0,0)E_{r,0}+\alpha(r,0)E_{2r,0}]+\gamma_0\alpha(r,0)E_{0,0}, \quad (88)$$

and

$$E_{r,(n+1)r}=\gamma_1[\alpha(0,0)E_{r,(n+1)r}+\alpha(r,0)E_{2r,(n+1)r}]+\gamma_0\alpha(r,0)E_{0,(n+1)r}. \quad (89)$$

We look for a solution of this system of difference equations of the form

$$E_{0,lr}=ae^{-ikl}+be^{ikl}, \quad (90)$$

where $l=1,2,3,\dots,n$,

$$E_{0,lr}=ce^{-ikl}+de^{ikl}, \quad (91)$$

where $l=-1,-2,-3,\dots$,

$$E_{lr,0}=e_0e^{-iql}+fe^{iql}, \quad (92)$$

where $l=1,2,\dots,l_0$,

$$E_{l_0r,lr}=e_0e^{-iq(l_0+l)}+fe^{iq(l_0+l)}, \quad (93)$$

where $l=1,2,3,\dots,n$,

$$E_{(l_0+1-l)r,(n+1)r}=e_0e^{-iq(l_0+n+l)}+fe^{iq(l_0+n+l)}, \quad (94)$$

where $l=1,2,\dots,l_0$,

$$E_{0,0}=h, \quad (95)$$

$$E_{0,(n+1)r}=h', \quad (96)$$

and

$$E_{0,lr}=re^{-ikl}+se^{ikl}, \quad (97)$$

where $l=n+2, n+3, n+4, \dots$. Substituting these forms in Eqs. (80)–(89) above, we find a system of ten algebraic equations that can be used to relate $a, b, c, d, e, f, h, h', r, s$ to one another.

An interesting case of these equations is to use them to relate the coefficients c, d to r, s . This then gives the transmission and reflection of the waveguide modes from the U loop. If we assume that the waveguide channel of the infinitely long channel and the U-shaped channel resonate at the same frequency (i.e., $\gamma_0=[\alpha(0,0)+2\alpha(r,0)\cos k]^{-1}$ and $\gamma_1=[\alpha(0,0)+2\alpha(r,0)\cos q]^{-1}$), then following a little algebra we find

$$\begin{vmatrix} c \\ d \end{vmatrix} = \begin{vmatrix} a_{11} & a_{12} \\ a_{12}^* & a_{11}^* \end{vmatrix} \begin{vmatrix} r \\ s \end{vmatrix}, \quad (98)$$

where

$$a_{11} = \frac{e^{-ik(n+1)}}{d_0} \left\{ \left(\frac{\sin k}{\sin k(n+1)} + \frac{\sin q}{\sin q(2l_0+n+1)} \right)^2 - \left(e^{ik} - \frac{\sin kn}{\sin k(n+1)} - \frac{\sin q(2l_0+n)}{\sin q(2l_0+n+1)} \right)^2 \right\}, \quad (99)$$

$$a_{12} = \frac{e^{ik(n+1)}}{d_0} \left\{ \left(\frac{\sin k}{\sin k(n+1)} + \frac{\sin q}{\sin q(2l_0+n+1)} \right)^2 - \left| e^{ik} - \frac{\sin kn}{\sin k(n+1)} - \frac{\sin q(2l_0+n)}{\sin q(2l_0+n+1)} \right|^2 \right\}, \quad (100)$$

and

$$d_0 = -2i \sin k \left(\frac{\sin k}{\sin k(n+1)} + \frac{\sin q}{\sin q(2l_0+n+1)} \right). \quad (101)$$

For there to be a unit transmitted flux in the region above the U loop, we need $r=0$ and $s=1$ in Eq. (98). The relative intensities of the incident and reflected flux in the region below the U loop are then $|a_{11}|^2$ and $|a_{12}|^2$, respectively.

In Fig. 4 we present results for the U-loop system with $n=l_0=10$. We plot the transmission coefficient, $T=1/|a_{11}|^2$, defined as the ratio of the transmitted to incident flux, versus the frequency ω in the stop gap. We use the parameters of the $\epsilon=9$, $R=0.37796a_c$ square lattice photonic crystal. The waveguide channels of the circuit are taken to have $t=0.01a_c$ with a nearest-neighbor impurity separation equal to the lattice constant of the square lattice. The reader is referred to the Appendix for a detailed discussion of the generation of the plots in Fig. 4 from the equations for the dispersion relations in the infinitely long channel, γ_0

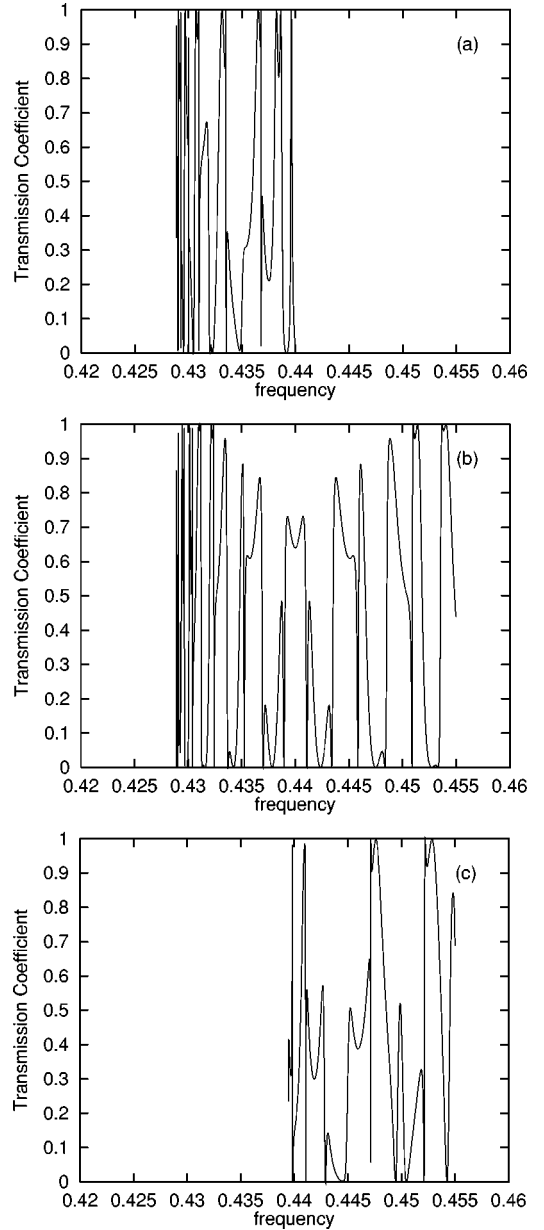


FIG. 4. Results for the U-loop problem. Plots for the transmission coefficient versus frequency in units of $\omega a_c/2\pi c$ are shown for $(q_c, k_c) =$ (a) $(\pi/2, \pi)$, (b) $(\pi/2, \pi/2)$, (c) $(\pi/2, \pi/10)$.

$=[\alpha(0,0)+2\alpha(1,0)\cos k]^{-1}$; the dispersion relations in the U loop, $\gamma_1=[\alpha(0,0)+2\alpha(1,0)\cos q]^{-1}$; and the transmission coefficient $T=1/|a_{11}|^2$.

As in our discussion of the dielectric barrier, we have chosen γ_0 and γ_1 in the plots in Fig. 4 so as to represent as diverse parameter space as possible in as few figures as possible. This is done by selecting them to fix a set of values of (q_c, k_c) , where q_c and k_c are the wave numbers in the U loop and the waveguide channel at the mid-stop-band frequency, $\omega a_c/2\pi c$. We have chosen $(q_c, k_c) = (\pi/2, \pi)$, $(\pi/2, \pi/2)$, $(\pi/2, \pi/10)$, respectively, for the plots in Figs. 4(a), 4(b), and 4(c). For these plots we have from Eq. (A3) $\gamma_0/\gamma_1 = 0.83, 1.00, \text{ and } 1.16$, respectively. For the frequency regions in which mode solutions are found in the system, we see that the transmission coefficient as a function of frequency exhibits an extremely complex behavior. All systems

display rapid oscillations between values near zero and values near one. This is due the phase interference between the waves traveling in the U loop and the waveguide upon their merger on the outgoing or transmitted wave side of the loop. The complex behavior of the transmission coefficient with frequency is unlike the transmission behavior in the waveguide barrier problem or in the problem of layered optical systems. In the barrier problem and the layered optical systems the transmission coefficient exhibits a periodic modulation as a function of frequency, related to the barrier length, which contains fewer number of harmonics than do the higher-dimensional (higher than one-dimensional) circuits such as that for the results in Fig. 4, possible in photonic crystal circuit systems. This is an interesting aspect of photonic circuits not seen in analogous electrical circuits where the transport is of a diffusive rather than a propagating wave nature.

Next let us consider the case of two infinitely long straight parallel waveguides that are joined by a short perpendicular channel. [See Fig. 2(d).] This is reminiscent of a branched system recently treated in Ref. 8. The impurity material forming the channels will be taken to be the same for all channels. The difference equations for this system are

$$E_{lr,0} = \gamma[\alpha(0,0)E_{lr,0} + \alpha(r,0)(E_{(l+1)r,0} + E_{(l-1)r,0})], \quad (102)$$

where $l = \pm 1, \pm 2, \pm 3, \dots$,

$$E_{lr,2r} = \gamma[\alpha(0,0)E_{lr,2r} + \alpha(r,0)(E_{(l+1)r,2r} + E_{(l-1)r,2r})], \quad (103)$$

where $l = \pm 1, \pm 2, \pm 3, \dots$,

$$E_{0,0} = \gamma[\alpha(0,0)E_{0,0} + \alpha(r,0)(E_{r,0} + E_{0,r} + E_{-r,0})], \quad (104)$$

$$E_{0,2r} = \gamma[\alpha(0,0)E_{0,2r} + \alpha(r,0)(E_{r,2r} + E_{0,r} + E_{-r,2r})], \quad (105)$$

and

$$E_{0,r} = \gamma[\alpha(0,0)E_{0,r} + \alpha(r,0)(E_{0,0} + E_{0,2r})]. \quad (106)$$

We assume a solution of the form

$$E_{lr,2r} = ae^{ikl} + be^{-ikl}, \quad (107)$$

where $l = 1, 2, 3, \dots$,

$$E_{lr,2r} = ce^{ikl} + de^{-ikl}, \quad (108)$$

where $l = -1, -2, -3, \dots$,

$$E_{lr,0} = ge^{ikl} + fe^{-ikl}, \quad (109)$$

where $l = -1, -2, -3, \dots$,

$$E_{lr,0} = he^{ikl} + ne^{-ikl}, \quad (110)$$

where $l = 1, 2, 3, \dots$,

$$E_{0,2r} = r_0, \quad (111)$$

$$E_{0,r} = s, \quad (112)$$

and

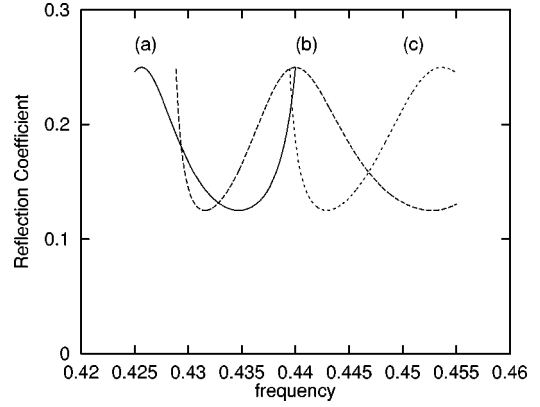


FIG. 5. Results from the parallel line problem. Plots for the reflection coefficient versus frequency in units of $\omega a_c/2\pi c$ are shown for $k_c =$ (a) π , (b) $\pi/2$, (c) $\pi/10$.

$$E_{0,0} = t. \quad (113)$$

Following a little algebra we find a matrix equation relating a, b, h, n to c, d, g, f ,

$$\begin{pmatrix} a \\ b \\ h \\ n \end{pmatrix} = \begin{pmatrix} a_{11} & a_{12} & a_{13} & a_{14} \\ a_{21} & a_{22} & a_{23} & a_{24} \\ a_{31} & a_{32} & a_{33} & a_{34} \\ a_{41} & a_{42} & a_{43} & a_{44} \end{pmatrix} \begin{pmatrix} c \\ d \\ g \\ f \end{pmatrix}, \quad (114)$$

where

$$a_{11} = \frac{\sin k[2 \sin 2k + i]}{2 \cos k(1 - \cos 2k)}, \quad (115)$$

$$a_{12} = \frac{i \sin k}{2 \cos k(1 - \cos 2k)}, \quad (116)$$

and $a_{11} = a_{22}^* = a_{33} = a_{44}^*$, $a_{12} = a_{13} = a_{14} = a_{21}^* = a_{23}^* = a_{24}^* = a_{31} = a_{32} = a_{34} = a_{41}^* = a_{42}^* = a_{43}^*$.

If a unit transmitted flux is present in the lower right-hand branch [See Fig. 2(d).] for an incident flux only in the lower left-hand branch, then $h = 1$, $n = 0$, $c = 0$, $b = 0$ in Eq. (114). Solving Eq. (114) for this case gives $a = f = d = -i/(i - 2 \sin 2k)$, $g = 2(i - \sin 2k)/(i - 2 \sin 2k)$. The relative intensity of the incident flux in the lower left branch is $|g|^2 = 4(1 + \sin^2 2k)/(1 + 4 \sin^2 2k)$. The relative intensity of the reflected flux in the lower left branch is $|f|^2 = 1/(1 + 4 \sin^2 2k)$. The relative transmitted intensity of flux in the upper branches is $|a|^2 = |d|^2 = 1/(1 + 4 \sin^2 2k)$. We find that $|g|^2 = |a|^2 + |d|^2 + |f|^2 + |h|^2$ so that the total energy flux is conserved in the network.

In Fig. 5 plots of the reflection coefficient in the lower left-hand branch, $R = |f/g|^2$, for a flux incident in the lower left-hand branch are shown as functions of ω . These plots are from the square lattice photonic crystal represented in Figs. 1, 3, and 4 and for waveguide channels with nearest-neighbor impurity separations equal to the lattice constant of the square lattice. We refer the reader to the Appendix for a more detailed discussion of the generation of Fig. 5 from the equations of the text. Results are presented for $\gamma = 0.342, 0.284, 0.244$ corresponding, respectively, to $k_c = \pi, \pi/2, \pi/10$ where we define k_c as in our previous plots in Fig. 3.

We see from Fig. 5 that the reflection from the circuit is strongly dependent on the frequency so that there are frequencies that minimize the reflection coefficient. At these frequencies the transmission to the lower right-hand branch is maximized. The results in Fig. 5(b) are particularly interesting as there are two frequencies corresponding to reflection minimum and two frequencies corresponding to reflection maxima.

As a final interesting case, we consider a closed-circuit waveguide that has a rectangular channel. The equations describing this system are

$$E_{r,lr} = \gamma[\alpha(0,0)E_{r,lr} + \alpha(r,0)(E_{r,(l+1)r} + E_{r,(l-1)r})], \quad (117)$$

where $l = 2, 3, \dots, n-1$,

$$E_{r,nr} = \gamma[\alpha(0,0)E_{r,nr} + \alpha(r,0)(E_{r,(n-1)r} + E_{2r,nr})], \quad (118)$$

$$E_{lr,nr} = \gamma[\alpha(0,0)E_{lr,nr} + \alpha(r,0)(E_{(l+1)r,nr} + E_{(l-1)r,nr})] \quad (119)$$

where $l = 2, 3, \dots, l_0 - 1$,

$$E_{l_0r,nr} = \gamma[\alpha(0,0)E_{l_0r,nr} + \alpha(r,0)(E_{(l_0-1)r,nr} + E_{l_0r,(n-1)r})], \quad (120)$$

$$E_{l_0r,lr} = \gamma[\alpha(0,0)E_{l_0r,lr} + \alpha(r,0)(E_{l_0r,(l+1)r} + E_{l_0r,(l-1)r})], \quad (121)$$

where $l = n-1, n-2, \dots, 2$,

$$E_{l_0r,r} = \gamma[\alpha(0,0)E_{l_0r,r} + \alpha(r,0)(E_{l_0r,2r} + E_{(l_0-1)r,r})], \quad (122)$$

$$E_{lr,r} = \gamma[\alpha(0,0)E_{lr,r} + \alpha(r,0)(E_{(l+1)r,r} + E_{(l-1)r,r})], \quad (123)$$

where $l = l_0 - 1, l_0 - 1, \dots, 2$,

$$E_{r,r} = \gamma[\alpha(0,0)E_{r,r} + \alpha(r,0)(E_{r,2r} + E_{2r,r})]. \quad (124)$$

Assuming a solution of the form

$$E_{r,lr} = ae^{-ikl} + be^{ikl}, \quad (125)$$

where $l = 1, 2, \dots, n$,

$$E_{lr,nr} = ae^{-ik(n+l-1)} + be^{ik(n+l-1)}, \quad (126)$$

where $l = 1, 2, 3, \dots, l_0$,

$$E_{l_0r,lr} = ae^{-ik(2n+l_0-l-1)} + be^{ik(2n+l_0-l-1)}, \quad (127)$$

where $l = 1, 2, \dots, n$, and

$$E_{lr,r} = ae^{-ik(2n+2l_0-l-2)} + be^{ik(2n+2l_0-l-2)}, \quad (128)$$

where $l = 1, 2, 3, \dots, l_0$, we find upon substitution in Eqs. (117)–(124) that the condition for modes to exist in the circuit is that $\gamma = [\alpha(0,0) + 2\alpha(r,0)\cos k]^{-1}$ and $k = N\pi/(n + l_0 - 2)$ where N is an integer.

V. CONCLUSIONS

We have studied the propagation of electromagnetic waves in various types of waveguide circuits in photonic crystals and have demonstrated that under certain conditions the mathematics describing this propagation can be reduced to a set of difference equations. The treatment is reminiscent of that of light in layered media,¹⁸ but the photonic waveguides and the richer topology they offer in their interconnection branching networks give them a more interesting physics than that of layered media. As we have seen in the text, the phase coherent effects in photonic circuits can cause the transmission and reflection coefficients of photonic circuits to be complicated functions of the mode frequencies. In addition, photonic circuits that have no input or output waveguide lines can exhibit a variety of bound state resonator modes that are tuned by the circuit geometry.

A feature of our theory is that very complicated and extended branching waveguide circuits can be treated and their physics is described by closed-form mathematical expressions involving elementary functions of mathematical physics. The photonic crystal circuits are described by a set of difference equations that can be quickly generated and solved. Using the evaluation techniques discussed in the Appendix, plots of the transmission and reflection coefficients, as well as the waveguide mode field geometries can be easily generated for a great variety of photonic circuits. This is also true in the study of the mode frequencies of resonant modes in closed-loop circuits.

An additional interesting physical feature of photonic crystal circuits is that they represent an optical analogy to electronic circuits. In electronic circuits, electrons diffuse through the network of the circuit. In photonic circuits, light propagates in a nondiffusive manner through the network. Consequently, the optical system exhibits a variety of interesting interference effects not seen in the energy transport in electronic circuits.

We hope that the simple models we have studied in this paper will be useful in understanding more complicated waveguide systems and systems formed from more general types of single-site impurities.

APPENDIX

In this appendix we show how some of the circuit models studied in this paper can be evaluated for a realization of a photonic crystal. We consider a two-dimensional photonic crystal, though the theory in the text is quite general and can handle both two- and three-dimensional photonic crystals. The two-dimensional photonic crystal we consider is an array of cylindrical rods of radius R , arranged on a square lattice of lattice constant, a_c , such that $R = 0.37796a_c$. The rods have dielectric constant $\epsilon = 9$ and are surrounded by vacuum. For electromagnetic waves propagating in the plane of the square lattice with an electric field vector polarized parallel to the axes of the rods, a stop band occurs for frequencies ω with $0.425 < \omega a_c / 2\pi c < 0.455$. (This particular photonic crystal and field polarization comprise the system used by us in Ref. 11 to illustrate the waveguide modes of an infinitely long waveguide in a two-dimensional photonic crystal and in Ref. 9 to present results on finite clusters of impurities in photonic crystals.)

In the circuit examples considered in the text, we take the waveguide channels to be oriented along the set of [10], [01] directions of the square lattice. Along these directions $\alpha(0,0)$ and $\alpha(1,0)$, for the photonic crystal described in the above paragraph, are dominant. Consequently, in the evaluation of the mathematical expression in this paper related to photonic circuits, $\alpha(0,0)$ and $\alpha(1,0)$ as functions of frequency in the stop bands are all that are needed. These can easily be obtained from the numerical results in Refs. 9 and 11.

As the stop bands of the photonic crystal generally extend over very narrow bands of frequencies, in any given stop band one finds to a good approximation

$$\alpha(0,0) = \alpha_c(0,0) + a_1(x - x_c) \quad (\text{A1})$$

and

$$\alpha(1,0) = \alpha_c(1,0) + b_1(x - x_c), \quad (\text{A2})$$

where $x = \omega a_c / 2\pi c$ ranges over the frequencies of the stop band, $x_c = \omega_c a_c / 2\pi c$ for ω_c the frequency at the center of the stop band, $\alpha_c(0,0)$ is the value of $\alpha(0,0)$ at ω_c , and $\alpha_c(1,0)$ is the value of $\alpha(1,0)$ at ω_c . For the model described in the previous paragraph with the $0.425 < x < 0.455$ stop band and for waveguides with $t = 0.01a_c$ we find to a very good approximation that, in units of a_c^2 , $\alpha_c(0,0) = 3.52$, $a_1 = 41.82$, $\alpha_c(1,0) = 0.300$, $b_1 = 6.03$, and $x_c = 0.440$. These parameters when used in the relation $\gamma = [\alpha(0,0) + 2\alpha(1,0)\cos k]^{-1}$ give

$$\gamma = \left\{ 3.52 + 41.82 \left(\frac{\omega a_c}{2\pi c} - 0.440 \right) + 2 \left[0.300 + 6.03 \left(\frac{\omega a_c}{2\pi c} - 0.440 \right) \right] \cos k \right\}^{-1}, \quad (\text{A3})$$

which reproduces the plot given in Fig. 4 of Ref. 11. [Note: In comparing the results from Eq. (A3) with the results in Fig. 4 of Ref. 11, it is important to note that Δ in the notation in Ref. 11 is the same as γ in the notation used in this paper.] These results are from fitting the numerical data in Ref. 11 for the $\alpha(r,s)$. As explained in Ref. 11 the results obtained there are computed from the numerical solutions for the modes of the photonic crystal and are essentially exact.

For the simple systems of Sec. III A, which consist of finite-length segments of waveguide, Eqs. (A1) and (A2) can be used directly in Eqs. (12), (15), and (16), or (20) to obtain the resonant modes. For fixed γ Eqs. (12), (15), and (16), or (20) with Eqs. (A1) and (A2) give the resonant frequencies found in the stop bands at which bound state modes are observed. Related types of cluster systems were treated by us in Ref. 9. We now discuss the more complicated circuit network geometries of Secs. III B and IV.

The circuits treated in this paper generally are formed from two or more different waveguide channels. For the discussions involving more than one waveguide channel, $\alpha(0,0)$ and $\alpha(1,0)$ often occur in expressions of the form

$$\gamma_0 = [\alpha(0,0) + 2\alpha(1,0)\cos k]^{-1} \quad (\text{A4})$$

for one waveguide channel and

$$\gamma_1 = [\alpha(0,0) + 2\alpha(1,0)\cos q]^{-1} \quad (\text{A5})$$

for a second waveguide channel. Equations (A4) and (A5) relate the dielectric parameters (i.e., through γ_0 and γ_1) in two different waveguide channels of a photonic circuit to the mode frequency, ω , which occurs in $\alpha(0,0)$ and $\alpha(1,0)$ and to the waveguide wave numbers k or q in each channel. [An example of this is the barrier problem in Sec. III B. In the barrier problem Eqs. (32) and (33) relate the dielectric constant in the waveguide channel and in the channel segment containing the barrier material to the mode frequency and wave number and are of the form of Eqs. (A4) and (A5) above.] The values of γ_0 and γ_1 , which give channel modes of frequency ω_c for wave numbers k_c and q_c are obtained from Eqs. (A4) and (A5) by evaluating $\alpha(0,0)$ and $\alpha(1,0)$ in Eqs. (A1) and (A2) at $x_c = \omega_c a_c / 2\pi c$. Once these values of γ_0 and γ_1 are fixed for given ω_c , q_c , k_c , then from Eqs. (A1)–(A5) we find

$$\cos k = \frac{-a_1(x - x_c) + 2\alpha_c(1,0)\cos k_c}{2[\alpha_c(1,0) + b_1(x - x_c)]} \quad (\text{A6})$$

and

$$\cos q = \frac{-a_1(x - x_c) + 2\alpha_c(1,0)\cos q_c}{2[\alpha_c(1,0) + b_1(x - x_c)]}, \quad (\text{A7})$$

where Eq. (A6) relates k to the mode frequency $\omega = 2\pi c x / a_c$ and Eq. (A7) relates q to the mode frequency $\omega = 2\pi c x / a_c$. Equations (A6) and (A7) relate k and q to ω for channels with fixed γ_0 and γ_1 . We shall now use the relations in Eqs. (A6) and (A7) to evaluate some of the photonic circuits considered in this paper.

1. Barrier

The case of a dielectric barrier in an infinitely long straight waveguide is treated in Eqs. (25)–(37) of the text. Equations (32) and (33) which give the dispersion in the waveguide and the barrier material have been discussed in Eqs. (A1)–(A7) above, and we will refer to these results in our discussion below.

For a unit incident flux on the barrier, the discussion in the text gives a transmission coefficient through the barrier from Eq. (37) of

$$T = \frac{2 \sin^2 k \sin^2 q}{(1 - \cos k \cos q)^2 + \sin^2 k \sin^2 q - (\cos q - \cos k)^2 \cos[(4n+2)q]} \quad (\text{A8})$$

and a reflection coefficient $R=1-T$. One can obtain a plot of T or R versus $\omega a_c/2\pi c$ by using Eqs. (A6) and (A7) to obtain k and q as a function of $\omega a_c/2\pi c$ for fixed k_c and q_c . The values k_c and q_c are fixed by Eqs. (A4) and (A5) so that

$$\cos k_c = \frac{1 - \gamma_0 \alpha_c(0,0)}{2 \gamma_0 \alpha_c(1,0)} \quad (\text{A9})$$

and

$$\cos q_c = \frac{1 - \gamma_1 \alpha_c(0,0)}{2 \gamma_1 \alpha_c(1,0)}, \quad (\text{A10})$$

where γ_0 and γ_1 are constants. Notice that γ_0 and γ_1 only depend on the values of the dielectric constant of the material forming the channel of the photonic crystal circuit and the fixed geometry of that material. Not all values of γ_0 and γ_1 will give solutions of Eqs. (A9) and (A10) for k_c and q_c .

2. Branched system

The branched system described in Eqs. (55)–(79) can be evaluated for the case in which $\gamma_0 = \gamma_1 = \gamma_2 = \gamma = [\alpha(0,0) + 2\alpha(1,0)\cos k]^{-1}$ by using Eqs. (A1)–(A7) to obtain k as a function of $\omega a_c/2\pi c$ for fixed $\gamma_0 = \gamma$ or k_c . We find the dispersion relation

$$\cos k = \frac{-a_1(x-x_c) + 2\alpha_c(1,0)\cos k_c}{2[\alpha_c(1,0) + b_1(x-x_c)]}, \quad (\text{A11})$$

where

$$\cos k_c = \frac{1 - \gamma \alpha_c(0,0)}{2 \gamma \alpha_c(1,0)}. \quad (\text{A12})$$

Once k is related to $\omega a_c/2\pi c$ through Eqs. (A11) and (A12) the reflection and transmission coefficients can be obtained from Eqs. (78) and (79) of the text.

3. U loop

In the U loop discussed in Eqs. (80)–(101) the values of γ_0 and k in the infinitely long waveguide channel are related by $\gamma_0 = [\alpha(0,0) + 2\alpha(1,0)\cos k]^{-1}$ and the values of γ_1 and q in the U loop are related by $\gamma_1 = [\alpha(0,0) + 2\alpha(1,0)\cos q]^{-1}$. These are essentially the same relationships encountered in the discussion given above for the barrier problem. The same discussion used for the barrier problem can be applied to these equations for the U-loop system to obtain k and q as functions of $\omega a_c/2\pi c$ from Eqs. (A6) and (A7). Once k and q are determined as functions of $\omega a_c/2\pi c$, Eqs. (99) and (100) of the text can be used to compute the transmission coefficient (i.e., $T=1/|a_{11}|^2$) and the reflection coefficient of a wave coming from infinity and incident on the U loop.

4. Two parallel waveguides with a connection

The system in Eqs. (102)–(116) can be treated by solving the relation $\gamma = [\alpha(0,0) + 2\alpha(1,0)\cos k]^{-1}$ for k as a function of $\omega a_c/2\pi c$ using the same approach discussed above for the branched system. Once k is known as a function of $\omega a_c/2\pi c$ the amplitudes of the waves in the various branches of the photonic circuit are given in terms of k . Specifically, from the discussions in the paragraph below Eq. (116) we have the reflection coefficient $R=1/4(1+4\sin^2 2k)$ and the transmission coefficients in each of the three lines leading away from the vertex $T=1/4(1+4\sin^2 2k)$.

*Fax: 616-387-4939. Electronic address: MCGURN@WMICH.EDU

¹J. D. Joannopoulos, R. D. Meade, and J. N. Winn, *Photonic Crystals* (Princeton University Press, Princeton, 1995).

²J. D. Joannopoulos, P. R. Villeneuve, and S. Fan, *Nature* (London) **386**, 143 (1997).

³A. A. Maradudin and A. R. McGurn, in *Photonic Band Gaps and Localization*, edited by C. M. Soukoulis (Plenum, New York, 1992), p. 247.

⁴R. D. Meade, A. Devenyi, J. D. Joannopoulos, O. L. Alerhand, D. A. Smith, and K. Kash, *J. Appl. Phys.* **75**, 4753 (1994).

⁵S. Fan, *J. Opt. Soc. Am. B* **12**, 1267 (1995).

⁶A. Mekis, *Phys. Rev. Lett.* **77**, 3787 (1996).

⁷A. Mekis, S. Fan, and J. D. Joannopoulos, *Phys. Rev. B* **58**, 4809 (1998).

⁸S. Fan, P. R. Villeneuve, J. D. Joannopoulos, and H. A. Haus, *Phys. Rev. Lett.* **80**, 960 (1998).

⁹H. G. Algul, M. Khazhinsky, A. R. McGurn, and J. Kapenga, *J.*

Phys.: Condens. Matter **7**, 447 (1995).

¹⁰A. R. McGurn and M. G. Khazhinsky, in *Photonic Band Gap Materials*, edited by C. M. Soukoulis (Kluwer Academic Press, Dordrecht, 1995), p. 487.

¹¹A. R. McGurn, *Phys. Rev. B* **53**, 7059 (1996).

¹²K. G. Khazhinsky and A. R. McGurn, *Phys. Lett. A* **237**, 175 (1998).

¹³A. R. McGurn, *Phys. Lett. A* **251**, 322 (1999).

¹⁴A. R. McGurn, *Phys. Lett. A* **260**, 314 (1999).

¹⁵M. Pihlal, A. Shambrook, A. A. Maradudin, and P. Sheng, *Opt. Commun.* **80**, 199 (1991).

¹⁶See *Photonic Band Gap Materials*, edited by C. M. Soukoulis (Kluwer, Dordrecht, 1996).

¹⁷D. Marcuse, *Theory of Dielectric Optical Waveguides*, 2nd ed. (Academic Press, Boston, 1995).

¹⁸P. Yeh, *Optical Waves in Layered Media* (Wiley, New York, 1988).